Kinetic Mechanism of *Escherichia coli* Isocitrate Dehydrogenase†

Antony M. Dean and Daniel E. Koshland, Jr.*

Department of Biological Chemistry, The Chicago Medical School, 3333 Green Bay Road, North Chicago, Illinois 60064-3095, and Department of Molecular and Cell Biology, University of California, Berkeley, California 94720

Received December 15, 1992; Revised Manuscript Received May 13, 1993®

ABSTRACT: The kinetic mechanism of the NADP-dependent isocitrate dehydrogenase of *Escherichia coli* was investigated using initial steady-state kinetic analyses. Kinetic coefficients, obtained using natural and alternative substrates with the wild-type and two mutant enzymes (S113L and S113N), suggest that the forward reaction [the oxidative decarboxylation of (2*R*,3*S*)-isocitrate by NADP] of the wild-type enzyme is a steady-state random mechanism, with catalysis more rapid than product release. The mechanism of the wild-type enzyme becomes rapid-equilibrium random when an alternative substrate [(2*R*)-malate or NAD] is used. The mutant enzymes always display rapid-equilibrium random kinetics, and for each enzyme the apparent dissociation constant of each substrate from the binary complex [K_{ia} = E·A/(EA)] is similar to its apparent dissociation constant from the Michaelis complex [K_a = (EB)·A/(EAB)], which suggests that the binding of one substrate is independent of the binding of the second. When the wild-type enzyme catalyzes the forward reaction, the apparent dissociation constant, K_{iIso}, is equal to its equilibrium dissociation constant, K_{dIso}, determined from equilibrium binding studies. However, the apparent dissociation constant of the cofactor, K_{iNADP}, is far smaller than its equilibrium dissociation constant, K_{dNADP}. This is consistent with the proposed mechanism, because simulations show that when catalysis is steady-state and product release is rate-limiting, K_{iNADP} and K_{NADP} will be far smaller than K_{dNADP}, while K_{iIso} and K_{Iso} remain similar to K_{dIso}. Product inhibition studies support the steady-state random mechanism of the wild-type enzyme. The rapid-equilibrium random mechanisms of the mutant enzymes provide evidence for the existence of E·Iso·NADPH and E·αKg·NADP abortive complexes and demonstrate that α-ketoglutarate and NADPH each bind to the free enzyme. Initial steady-state rate and product inhibition studies of the reverse reaction indicate a random addition of α-ketoglutarate and NADPH, with CO_2 possibly binding last. Dead-end inhibition studies, using tricarballylate (propane-1,2,3-tricarboxylic acid) as an analog of isocitrate and adenosine 2′,5′-diphosphate as an analog of NADP, are incompatible with ordered mechanisms in either direction.

Recent crystallographic and kinetic studies of the NADP-dependent isocitrate dehydrogenase [(2*R*,3*S*)-isocitrate: $NADP^+$ oxidoreductase (decarboxylating); EC 1.1.1.42] of *Escherichia coli* have elucidated the mechanism by which phosphorylation regulates this enzyme (Hurley *et al.*, 1990; Dean & Koshland, 1990). Phosphorylation of a serine in the active site inactivates *E. coli* isocitrate dehydrogenase (IDH) by preventing substrate binding through the direct steric blocking and the electrostatic repulsion of the γ-carboxylate of isocitrate. The crystal structure of native *E. coli* IDH with bound isocitrate is consistent with much previous work on the catalytic mechanism of IDH from other species (Steinberger & Westheimer, 1951; Siebert *et al.*, 1957; Lienhard & Rose, 1964; Londesborough & Dalziel, 1968; Erhlich & Colman, 1987; Grissom & Cleland, 1988; Hurley *et al.*, 1991). This is postulated to occur in two steps, with dehydrogenation preceding decarboxylation:

$$\text{isocitrate}^{3-} + \text{NADP}^+ \overset{Mg^{2+}}{=} \text{oxalosuccinate}^{3-} + \text{NADPH} + \text{H}^+$$

$$\text{oxalosuccinate}^{3-} + \text{H}^+ \overset{Mg^{2+}}{=} \alpha\text{-ketoglutarate}^{2-} + \text{CO}_2$$

All known IDHs have an absolute requirement for a divalent metal cation, such as magnesium. In the *E. coli* IDH structure, magnesium is coordinated between the carboxylate and hydroxyl groups of the α-carbon of isocitrate, where it is in a position to stabilize negative charges formed on the hydroxyl oxygen during the transition states of both steps (Steinberger & Westheimer, 1951; Hurley *et al.*, 1991).

In contrast to the 48–58% sequence identity between the (2*S*)-malate dehydrogenases of the eukaryotic mitochondrion and *E. coli* (Thompson *et al.*, 1988), there is no sequence identity between *E. coli* IDH and the mitochondrial NADP-dependent IDH of *Saccharomyces cerevisiae* (Haselbeck & McAlister-Henn, 1991). The *S. cerevisiae* IDH contains the Gly-X-Gly-X-X-Gly consensus sequence of the nucleotide binding site of a Rossmann fold (Rossmann *et al.*, 1974), but the *E. coli* enzyme has no such sequence and its crystal structure reveals no analogous domain (Hurley *et al.*, 1989, 1991). The lack of sequence identity suggests that eukaryotic mitochondrial and prokaryotic IDHs have separate evolutionary histories.

Although dissimilar enzymes may adopt similar catalytic mechanisms through convergent evolution, there is no known *a priori* requirement that they must adopt similar kinetic mechanisms. The intensively studied eukaryotic mitochondrial NADP-dependent IDHs from pig heart (Uhr *et al.*, 1974; Northrop & Cleland, 1974) and from beef heart (Londesborough & Dalziel, 1970) have steady-state random mechanisms. Another eukaryotic IDH from the digestive gland of the mussel *Mytilus edulis* displays rapid-equilibrium random kinetics (Head, 1980). In all three cases, various abortive complexes form. In contrast, a steady-state ordered mechanism (NADP binds first and isocitrate binds second; products

† This work was supported by the Lucille P. Markey Charitable Trust and by National Science Foundation Grant 04200 to D.E.K.
® Abstract published in *Advance ACS Abstracts,* August 15, 1993.

0006-2960/93/0432-9302$04.00/0

are released in the order CO_2, α-ketoglutarate, and then NADPH; an abortive E·NADP·αKg complex forms) has been proposed for both the *E. coli* and the *Rhodopseudomonas sphaeroides* enzymes (Nimmo, 1986; Buzdygon *et al.*, 1973). This suggests that the eukaryotic and prokaryotic IDH enzymes may have different kinetic mechanisms despite a common catalytic chemistry and increases the importance of rigorously determining the mechanism for the *E. coli* enzyme.

The demonstration that isocitrate and NADP each bind to the free enzyme from *E. coli* (Dean *et al.*, 1989) does not prove that the kinetic mechanism is random, because one of the enzyme substrate complexes could be abortive. Rapid-equilibrium random mechanisms have been proposed for the IDH of *Azobacter vinelandii*, where two ternary abortive complexes form and the release of products is in the order CO_2, α-ketoglutarate, and then NADPH (Wicken *et al.*, 1972), and the IDH of *Salmonella typhimurium* (a close relative of *E. coli*), in which the absence of abortive complexes seems rather peculiar (Marr & Weber, 1973). These conflicts were sufficient to warrant a more detailed investigation of the kinetic mechanism of the NADP-dependent IDH of *E. coli*. Here, studies using product inhibitors, dead-end inhibitors, alternate substrates, and site-directed mutants of the enzyme are used to elucidate the kinetic mechanism of the IDH of *E. coli*. It turns out that all of those enzymes studied in extensive detail have steady-state random mechanisms, even though the primary sequences have no resemblance and the IDH *E. coli* enzyme has no Rossmann fold. Apparently there has been a convergent evolution for kinetic mechanisms, and the different structures can now be examined to identify the structural features which create this coenzyme.

MATERIALS AND METHODS

Materials. Strains, growth conditions, site-specific mutagenesis, enzyme purifications, and protein determinations were as previously described (Dean *et al.*, 1989; Dean & Koshland, 1990).

Electrophoresis. SDS–polyacrylamide electrophoresis followed by staining with Coomassie blue was used to determine the purity of the enzyme preparations. Following native polyacrylamide gel electrophoresis of purified mutant enzymes, gels were stained for protein content using Coomassie blue and for dehydrogenase activity by coupling the production of NAD(P)H to the reduction of nitro blue tetrazolium and phenazine methosulfate (0.1 M Tris-HCl, pH 7.6, with 0.25 mM nitro blue tetrazolium and 0.078 mM phenazine methosulfate, 1 mM NAD or NADP, and either 1 mM D,L-isocitrate or 50 mM (2*R*)-malate or 50 mM (2*S*)-malate, in the presence of 5 mM free Mg^{2+}) (Reeves *et al.*, 1972) which precipitate as blue bands.

Chelation Assays. The equilibrium dissociation constants from the magnesium–substrate and magnesium–nucleotide complexes were determined using the method of Burton (1959) by spectrophotometric measurement at 360 nm of the complex formed between 8-hydroxyquinoline and magnesium in KAC buffer (25 mM MOPS, 100 mM NaCl, and 1 mM dithiothreitol, pH 7.3) at 21 °C.

Kinetics Assays. The kinetics of isocitrate dehydrogenases were determined in KAC buffer at 21 °C in the presence of 5 mM free Mg^{2+} in the assay solutions and added as $MgCl_2$, the quantity determined using the dissociation constants shown in Table I. Data were collected on a Hewlett-Packard 8452A single-beam diode array spectrophotometer which is capable of measuring reaction rates as low as 0.002 Δ_{340nm}/min. Given sufficient time (usually about 30 min), rates as low as 6×10^{-6} Δ_{340nm}/min can be measured using repeated blanking with internal referencing at 440 nm. The rates of reaction were determined by monitoring the production or consumption of NAD(P)H at 340 nm in a 1-cm light path. The concentration of NAD(P)H was determined using a molar extinction coefficient of 6200 Δ_{340nm}/cm. Fresh solutions of $NaHCO_3$, which had been adjusted to pH 7.3 and kept in stoppered bottles, were added to the reaction mixtures immediately before the addition of the enzyme. At 21 °C, pH 7.3, the total bicarbonate is partitioned into 89% HCO_3^- and 11% CO_2, with the latter being the true substrate for the enzyme (Londesborough & Dalziel, 1968). For initial velocity studies, the concentration of one substrate was varied at several fixed levels of the second substrate, and for the reverse reaction the concentration of the third substrate was varied as well. Protein concentrations were determined at 280 nm using a molar extinction coefficient of 66 330 Δ_{280nm}/cm (Dean *et al.*, 1989).

Table I: Dissociation Constants of Mg^{2+}–Ligand Complexes Used for Calculating Free Mg^{2+} [a]

ligand	pK_d	published pK_d	source
(2*R*,3*S*)-isocitrate	2.1	3.2	Duggleby and Dennis (1970)
		2.3	Northrop and Cleland (1974)
		3.1	Willson and Tipton (1981)
		2.2	Grissom and Cleland (1988)
α-ketoglutarate	1.5	1.6	Northrop and Cleland (1974)
(2*R*)-malate	1.6	1.6	Dawson *et al.* (1969)
tricarballylate	1.5		
NADP	3.0	1.7	Apps (1973)
NAD	2.1	2.0	Duggleby and Dennis (1970)
		1.7	Apps (1973)
adenosine 2′,5′-diphosphate	2.7		

[a] Data were obtained in 25 mM MOPS, 100 mM NaCl, 1 mM dithiothreitol, and 1 mM 8-hydroxyquinoline, pH 7.3 at 21 °C. pK_d = $\log_{10}$([free ligand][free enzyme]/[bound ligand]. Standard errors are less than 12.5% of the estimates.

Data Analyses. Weighted nonlinear least-squares Marquardt regressions were used to determine the fit of complete kinetics data sets to the following models. Following the notation of Cleland (1963)

initial steady-state rate bi mechanism

$$v = VAB/(K_{ia}K_b + K_aB + K_bA + AB) \quad (1)$$

where A and B are the substrate concentrations, v is the velocity, V is the maximum velocity, K_{ia} is the apparent dissociation constant of the E·A binary complex (E·A ↔ E + A), and K_a and K_b are the Michaelis constants for A and B from the E·A·B ternary complex. The Michaelis constants are dissociation constants from central complexes only in a rapid-equilibrium mechanism where catalysis and/or first product release are rate-limiting. The equations describing the effects of an inhibitor I are

linear competitive inhibition

$$v = VA/[K(1 + I/K_{is}) + A] \quad (2)$$

linear uncompetitive inhibition

$$v = VA/[K + A(1 + I/K_{ii})] \quad (3)$$

linear noncompetitive inhibition

$$v = VA/[K(1 + I/K_{is}) + A(1 + I/K_{ii})] \quad (4)$$

where K is the apparent Michaelis constant of the substrate

Table II: Kinetic Constants from Initial Rate Studies[a]

	enzyme								
	S113			S113N			S113L		
substrate	K_i (mM)	K_m (mM)	k_{cat} (s^{-1})	K_i (mM)	K_m (mM)	k_{cat} (s^{-1})	K_i (mM)	K_m (mM)	k_{cat} (s^{-1})
				Forward Reactions					
isocitrate	0.004	0.011	80.5	0.017	0.018	3.85	0.066	0.025	0.36
NADP	0.006	0.017		0.275	0.291		0.464	0.176	
malate	1.4	2.1	0.0082	20.8	16.5	0.00067	5.3	5.2	0.00047
NADP	0.132	0.195		0.296	0.234		0.412	0.420	
isocitrate	0.004	0.006	3.22	0.021	0.119	0.0092	0.074	0.103	0.00067
NAD	2.7	4.7		2.72	15.3		5.9	4.3	
				Reverse Reaction Catalyzed by Wild-Type S113 Enzyme[b]					
$K_{\alpha Kg}$	0.57 mM	(coeff αKg)		0.522 mM^2	constant of eq 5		0.15 mM^3	k_{cat}	14.9 s^{-1}
K_{NADPH}	0.007 mM	(coeff NADPH)		4.18 mM^2					
K_{CO_2}[d]	3.13 mM	(coeff CO_2[d])		0.052 mM^2					

[a] Data were obtained in 25 mM MOPS, 100 mM NaCl, 5 mM free Mg^{2+}, and 1 mM dithiothreitol, pH 7.3 at 21 °C. Estimates were obtained using a weighted least-squares Marquardt nonlinear regression. All apparent standard errors are less than 15% of the estimates. [b] Terms calculated from eq 5 in reciprocal form. [c] αKg = α-ketoglutarate. [d] Concentration given in terms of total bicarbonate.

whose concentration is varied and K_{is} and K_{ii} are the slope and intercept inhibition constants (Cleland, 1963). There is a complementary set of equations describing the effects of the inhibitor when the concentration of B is varied and the concentration of A is fixed.

In the notation of Cleland (1982), the general form for a Ter rate equation is

$$v = VPQR/[\text{constant} + (\text{coeff P})P + (\text{coeff Q})Q + (\text{coeff R})R + K_pQR + K_qPR + K_rPQ + PQR] \quad (5)$$

where the coefficients of P, Q, and R are mechanism-dependent (Cleland, 1982). The double reciprocal transformation was used to fit eq 5 by the method of least squares using a least-squares algorithm available in the software Mathematica, with weights proportional to v^2.

RESULTS

Enzyme Purity. Electrophoresis of purified wild-type and mutant IDHs reveals a single band in each lane when stained with Coomassie blue, indicating that the preparations are substantially free of contaminating protein. Staining for NADP-dependent IDH activities following native polyacrylamide gel electrophoresis (Dean & Koshland, 1990) reveals a single band in the same position in each lane. Duplicate gels, stained in the presence of isocitrate and NAD or (2*R*)-malate and NADP, produced identical banding patterns. Hence, *E. coli* IDH can utilize NAD or (2*R*)-malate as alternative substrates.

When native polyacrylamide gels are stained for activity toward (2*R*)-malate with NAD as the cofactor, a new band with a lower relative mobility appears and no bands congruent with IDH are detected. A duplicate gel stained for activity with (2*S*)-malate and NAD reveals darker bands which are congruent with those at the lower relative mobility position. Since (2*R*)-malate is contaminated with a small quantity of (2*S*)-malate (less than 0.5%), it seems likely that IDH preparations are contaminated with an NAD-dependent (2*S*)-malate dehydrogenase activity.

Metal Chelation. The method of Burton (1959) was used to determine the equilibrium dissociation constants of the magnesium–nucleotide and magnesium–substrate complexes in conditions that were identical to those used in the kinetics studies. The results (Table I) agree with those published in the literature, and the small differences can be ascribed to different experimental conditions, different experimental procedures, and experimental errors. Estimates of the equilibrium dissociation constants were used to determine the quantity of $MgCl_2$ to add to bring the concentration of free Mg^{2+} to 5 mM for the kinetic assays.

Kinetic Results. Estimates of the kinetic parameters are presented in Tables II and III. Despite Michaelis constants in the low micromolar range for the wild-type enzyme utilizing the natural substrates, initial steady-state rates remain proportional to the concentration of enzyme present and remained linear for at least 60 s. Measurements of the very low rates associated with the alternate substrates, (2*R*)-malate or NAD, are only possible because the initial steady-state rates, even at the lowest concentrations of substrates used, remain linear for at least 10 min. Although the reverse reaction is not thermodynamically favored, initial steady-state rates were proportional to the concentration of enzyme added and remained linear for at least 100 s. The standard errors are generally less than 15% of the estimates. Partial regression analyses were used to distinguish between the kinetic models and the residuals were inspected for systematic biases.

Substrate inhibition often provides a helpful tool for distinguishing kinetic mechanisms (Cleland, 1979). In the forward reaction, no evidence for substrate inhibition by isocitrate or NADP was detectable up to 50-fold above the apparent binding constants. In the reverse reaction, substrate inhibition by CO_2 was detected at concentrations exceeding 7.3 mM, which corresponds to a total bicarbonate concentration of 80 mM (data not shown). Inhibition seen at such high concentrations of bicarbonate is of no diagnostic value because bicarbonate, changes in sodium ion concentration, and changes in ionic strength may be inhibitory. There is no evidence of substrate inhibition by NADPH or α-ketoglutarate within the ranges of concentrations used (0.01–0.08 mM for NADPH and 0.5–16 mM for α-ketoglutarate). This does not exclude the possibility of substrate inhibition at higher concentrations of these substrates, particularly for α-ketoglutarate, which yields strong substrate inhibition with the mammalian enzyme (Uhr *et al.*, 1974). However, the concentrations of α-ketoglutarate necessary to detect substrate inhibition with the *E. coli* enzyme are sufficiently large that inhibitory effects caused by concomitant changes in sodium ion concentration and ionic strength are likely.

A test of the quality of the data for wild-type S113 enzyme with the natural substrates is provided by the Haldane relation for a completely random bi-ter, $K_{eq} = (V_{max,f}/K_{iIso}/K_{NADP})/$

Table III: Kinetic Constants from Inhibition Studies[a]

enzyme	varied substrate[b]	inhibitor	pattern	K_{is}[a] (mM)	K_{ii}[a] (mM)	fixed substrates	concns[d] (mM)
S113	Iso	αKg	NC	5.1 ± 1.1	9.6 ± 0.72	NADP	0.028
	Iso	NADPH	NC	0.015 ± 0.003	0.131 ± 0.024	NADP	0.040
	NADP	αKg	NC	6.09 ± 2.29	4.76 ± 0.44	Iso	0.027
	NADP	NADPH	NC	0.020 ± 0.002	0.169 ± 0.018	Iso	0.027
	Iso	Tca	C	3.38 ± 0.44		NADP	0.020
	Iso	A2′5′DP	NC	0.48 ± 0.04	1.69 ± 0.24	NADP	0.021
	NADP	Tca	NC	8.21 ± 0.85	14.62 ± 0.97	Iso	0.017
	NADP	A2′5′DP	NC	0.65 ± 0.06	2.78 ± 0.09	Iso	0.020
	αKg	Iso	C	0.011 ± 0.001		NADPH, CO_2	0.013, 17.0[e]
	αKg	NADP	NC	0.019 ± 0.004	0.145 ± 0.042	NADPH, CO_2	0.023, 17.0
	NADPH	Iso	NC	0.005 ± 0.001	0.05 ± 0.02	αKg, CO_2	0.5, 16.0
	NADPH	NADP	C	0.019 ± 0.002		αKg, CO_2	2.2, 17.0
	αKg	Tca	NC	5.09 ± 1.69	22.55 ± 2.23	NADPH, CO_2	0.026, 16.0
	αKg	A2′5′DP	NC	2.97 ± 0.70	7.3 ± 2.3	NADPH, CO_2	0.013, 17.0
	NADPH	Tca	NC	5.89 ± 1.15	27.06 ± 5.5	αKg, CO_2	0.5, 16.0
	NADPH	A2′5′DP	C	0.465 ± 0.048		αKg, CO_2	0.5, 32.0
	Mal	αKg	C	0.225 ± 0.026		NADP	0.11
	Mal	NADPH	NC	0.039 ± 0.04	0.025 ± 0.008	NADP	0.23
	NADP	αKg	NC	0.187 ± 0.051	0.94 ± 0.17	Mal	1.56
	NADP	NADPH	C	0.015 ± 0.001		Mal	0.53
	Iso	αKg	C	3.16 ± 0.31		NAD	1.25
	Iso	NADPH	NC	0.013 ± 0.003	0.053 ± 0.005	NAD	2.5
	NAD	αKg	NC	4.06 ± 0.96	16.25 ± 4.44	Iso	0.005
	NAD	NADPH	C	0.014 ± 0.02		Iso	0.039
S113L	Iso	αKg	C	5.13 ± 0.41		NADP	0.156
	Iso	NADPH	NC	0.045 ± 0.003	0.653 ± 0.089	NADP	0.156
	NADP	αKg	NC	5.75 ± 1.03	14.8 ± 3.24	Iso	0.02
	NADP	NADPH	C	0.047 ± 0.007		Iso	0.038
	Iso	Tca	C	3.44 ± 0.33		NADP	0.156
	Iso	A2′5′DP	NC	0.099 ± 0.01	0.159 ± 0.011	NADP	0.156
	NADP	Tca	NC	6.03 ± 0.54	17.9 ± 2.64	Iso	0.02
	NADP	A2′5′DP	C	0.075 ± 0.012		Iso	0.038
S113N	Iso	αKg	C	7.71 ± 2.08		NADP	0.313
	Iso	NADPH	NC	0.034 ± 0.004	0.186 ± 0.011	NADP	0.080
	NADP	αKg	NC	6.93 ± 1.03	26.53 ± 4.53	Iso	0.019
	NADP	NADPH	C	0.019 ± 0.003		Iso	0.019

[a] Data were obtained in 25 mM MOPS, 100 mM NaCl, 5 mM free Mg^{2+}, and 1 mM dithiothreitol, pH 7.3 at 21 °C. Estimates were obtained using a weighted least-squares Marquardt nonlinear regression. [b] Iso, (2*R*,3*S*)-isocitrate; Mal, (2*R*)-malate; αKg, α-ketoglutarate; Tca, tricarballylate; A2′5′DP, adenosine, 2′,5′-diphosphate. [c] C, competitive inhibition; NC, noncompetitive inhibition. [d] Concentrations are for total inhibitor in the presence of 5 mM Mg^{2+}. [e] Concentration of CO_2 is given as total bicarbonate added.

[(constant/$V_{max,r}$)(CO_2/total bicarbonate)], where *f* and *r* designate the forward and reverse reactions, the constant term is determined from eq 5, and the factor CO_2/total bicarbonate = 0.11 (Londesborough & Dalziel, 1968). K_{eq} = 1380 mM, obtained using the estimates in Table II, is in remarkably good agreement with the estimates of 930 mM (Londesborough & Dalziel, 1968) and 1140 mM (Uhr *et al.*, 1974). This gives confidence that the kinetic data are not significantly compromised by the initial production of products.

DISCUSSION

Forward Reaction. Initial rate data for the oxidative decarboxylation of (2*R*,3*S*)-isocitrate by NADP using the wild-type S113 enzyme produce double-reciprocal plots with significant slope and intercept effects regardless which substrate is considered "fixed" (Figure 1). Initial steady-state rate studies, using (2*R*)-malate and NADP or (2*R*,3*S*)-isocitrate and NAD, yield similar linear intersecting patterns on double-reciprocal plots (Figure 1), as do initial steady-state rate studies with two mutant enzymes, S113L and S113N. Such patterns are consistent with both steady-state ordered and random bi mechanisms (Cleland, 1970), and in each case a nonlinear regression to the sequential bi model described by eq 1 provides an adequate fit to the data (Table II). Fits to the ping-pong and rapid-equilibrium ordered mechanisms are significantly worse, with the residuals displaying systematic biases.

Equilibrium binding studies demonstrate that the wild-type and several mutant enzymes can bind isocitrate and NADP (Dean *et al.*, 1989). An ordered mechanism would require one of the binary complexes, E·NADP or E·Iso, to be abortive. Yet neither NADP nor isocitrate produces detectable substrate inhibition up to 50-fold above its apparent binding constant. Consequently, an ordered kinetic mechanism with an abortive binary complex is unlikely. This suggests that the kinetic mechanism of the wild-type S113 enzyme is random.

The proposed random mechanism is illustrated in Figure 2 (mechanism A) together with the kinetic constants and equilibrium binding constants. When the K_i values from initial velocity patterns with NADP (mechanism A) or NAD (mechanism B) are compared, the K_{iIso} is identical and matches the dissociation constant of 0.005 mM determined in equilibrium binding studies (Dean *et al.*, 1989). Conversely, the K_{iNADP} values with (2*R*,3*S*)-isocitrate (mechanism A) and (2*R*)-malate (mechanism C) differ, and only that with malate matches the dissociation constant of 0.125 mM in equilibrium binding studies. This suggests that the wild-type S113 enzyme displays rapid-equilibrium random kinetics when (2*R*)-malate is the substrate but that K_{iNADP} is far lower than expected during the faster reaction with isocitrate.

That IDH has a random mechanism receives support from initial rate studies with the two mutant enzymes. Site-directed mutagenesis was used to replace S113, which normally hydrogen-bonds to the γ-carboxylate of isocitrate (Hurley *et al.*, 1990), thereby reducing the rate of catalysis by factors

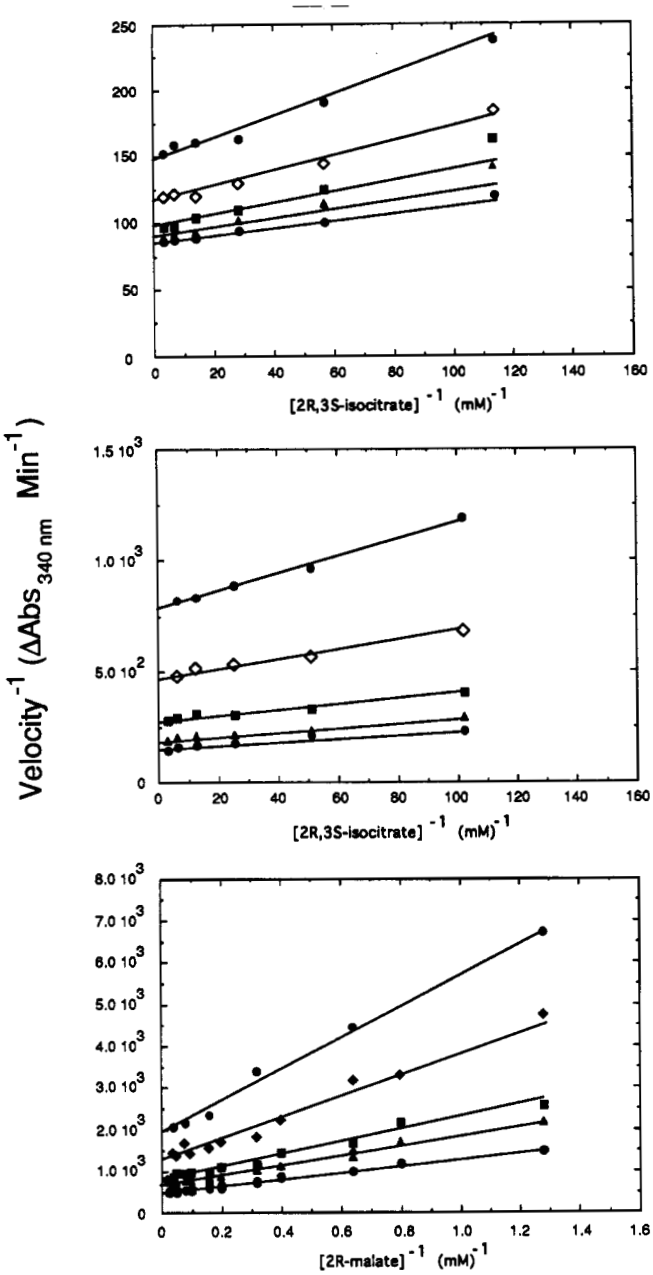

FIGURE 1: Initial steady-state rate kinetics for oxidative decarboxylation reactions catalyzed by the wild-type S113 enzyme. Substrates are (top panel) (2*R*,3*S*)-isocitrate with NADP at (○) 0.021, (◆) 0.042, (▲) 0.084, (■) 0.168, and (●) 0.336 mM; (middle panel) (2*R*,3*S*)-isocitrate with NAD at (○) 0.63, (◆) 1.25, (▲) 2.5, (■) 5.0, and (●) 10.0 mM; and (bottom panel) (2*R*)-malate with NADP at (○) 0.04, (◆) 0.078, (▲) 0.156, (■) 0.325, and (●) 0.625 mM. All assays were conducted in a buffer of 25 mM MOPS, 100 mM NaCl, 5 mM free Mg^{2+}, and 1 mM dithiothreitol, pH 7.3 at 21 °C.

of 100 and 50 for the S113L and S113N substitutions, respectively (mechanisms D and E, Figure 2). A comparison of the kinetic constants obtained from initial rate studies using isocitrate or (2*R*)-malate with NADP and isocitrate with NAD reveals that the only kinetic parameters which remain constant for each enzyme are the dissociation constants K_{iIso} and K_{iNADP} (Table II). Such a result is expected for rapid-equilibrium random mechanisms (Huang, 1979).

Simulations of the faster reaction of the wild-type S113 enzyme utilizing isocitrate and NADP show that a random mechanism operating at steady-state is capable of reducing the K_{iNADP} compared to K_{dNADP} while retaining the equality between K_{iIso} and K_{dIso} (mechanism F, Figure 2). The substrates are assumed to have identical affinities for the free enzyme and the binary complexes because the dissociation constants are rather similar to the Michaelis constants in the rapid-equilibrium reactions (Table II, mechanisms B–E in Figure 2). The on rates of the natural substrates are assumed to be identical and equal to 8×10^6/M/s. The off rates, determined as the products of the equilibrium dissociation constants with the on rates, are 40/s for isocitrate and 1000/s for NADP. Catalysis (rate = 1700/s) is faster than the off rate of either substrate from the Michaelis complex, and unlike previous simulations of the random bi mechanism (Rudolph & Fromm, 1971), a second rate-limiting step downstream from catalysis (rate = 85/s) has been introduced to prevent K_{NADP} from exceeding the equilibrium dissociation constant. An exact symbolic solution to the set of simultaneous equations describing mechanism F in Figure 2 was obtained using Mathematica software.

The simulated kinetic constants in mechanism F compare favorably with those determined experimentally. The simulated k_{cat} is identical to the experimental value, the drastic reduction in K_{iNADP} compared with K_{dNADP} is faithfully reproduced without noticeably affecting K_{iIso}, and double-reciprocal plots yield the linear intersecting patterns typical of a random bi mechanism (not shown). Although mechanism F adequately explains the data, the full steady-state random bi-ter mechanism, with or without abortive complexes, has a sufficiently complicated rate equation that other explanations are not definitively excluded. Nevertheless, results from both experiment and simulation are consistent with the notion that wild-type IDH has a steady-state random kinetic mechanism which can be brought into rapid equilibrium through reductions in maximum velocity caused by site-directed mutagenesis or through the use of alternate substrates.

Studies using NADPH and α-ketoglutarate as product inhibitors provide additional support for a steady-state random mechanism. The wild-type S113 enzyme produces four noncompetitive patterns (Table III). Simulations of a steady-state random bi-bi with abortive complex formation show that all product inhibition patterns can be noncompetitive over a wide range of conditions (Rudolph & Fromm, 1971). The behavior of a steady-state random bi-ter with abortive complexes (Figure 3) will be similar because the random bi-bi is a subset of the random bi-ter scheme. Theoretically, the inhibition patterns are nonlinear, although the curvature is difficult to detect when the initial steady-state rate patterns appear linear (Rudolph & Fromm, 1971). Thus, the four noncompetitive patterns, obtained when α-ketoglutarate and NADPH are used to inhibit the forward reaction with the natural substrates (Table III), are consistent with a steady-state random bi mechanism with the formation of at least one abortive complex (E·Iso·NADPH and/or E·αKg·NADP, Figure 3).

Direct evidence for abortive complex formation is provided by the product inhibition studies of the rapid-equilibrium reactions. For the S113L and S113N mutant enzymes, α-ketoglutarate is a competitive inhibitor of (2*R*,3*S*)-isocitrate and a noncompetitive inhibitor of NADP, while NADPH is a competitive inhibitor of NADP and a noncompetitive inhibitor of (2*R*,3*S*)-isocitrate (Table III). The wild-type enzyme produces similar inhibition patterns with either alternative substrate, (2*R*)-malate or NAD (Table III). Such inhibition patterns are typical of rapid-equilibrium random mechanisms with two abortive complexes. Thus, E·Iso·NADPH and E·αKg·NADP can form on the wild-type S113 and the mutant S113L and S113N enzymes.

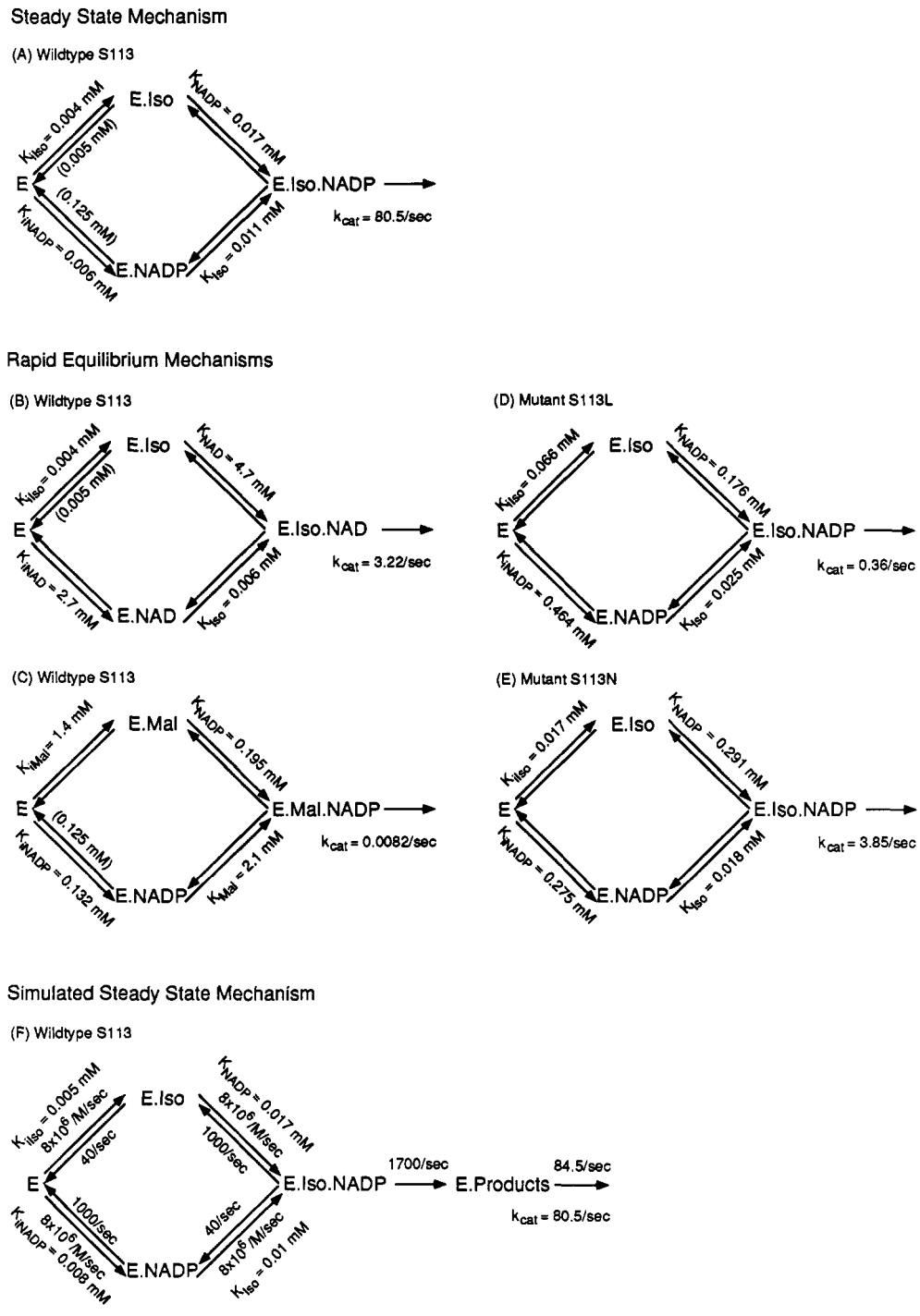

FIGURE 2: Proposed random mechanisms of the forward reactions. (A) Steady-state mechanism of the wild-type S113 enzyme utilizing isocitrate (Iso) and NADP, presented with the kinetic constants from Table II with the equilibrium binding constants in parentheses. Rapid-equilibrium random mechanisms: the wild-type S113 enzyme utilizing isocitrate and NAD (B) and (2*R*)-malate (Mal) and NADP (C) and the mutant enzymes S113L (D) and S113N (E) utilizing isocitrate and NADP. (F) Simulation of the steady-state random mechanism of the wild-type S113 enzyme utilizing isocitrate and NADP. The on rates of the natural substrates are assumed to be identical and equal to $8 \times 10^6/M/s$, and the off rates are 40/s for isocitrate and 1000/s for NADP, so that the dissociation constants of both substrates to the free enzyme and the binary complexes are equal to those obtained in the equilibrium binding experiments. Distal to the catalytic step (rate = 1700/s, which is faster than the off rates of either substrate) is a second rate-limiting step (step = 85/s). The simulation faithfully reproduces the kinetic constants and maximum velocity observed in mechanism A.

Tricarballylate (propane-1,2,3-tricarboxylic acid), an analog of isocitrate, and adenosine 2′,5′-diphosphate, an analogue of NADP, were used as dead-end inhibitors. The S113L mutant enzyme yields the two competitive and two noncompetitive inhibition patterns expected of a rapid-equilibrium random mechanism with two abortive complexes (Table III). Similar results are obtained with the wild-type enzyme utilizing the natural substrates, except that the inhibition of NADP by adenosine 2′,5′-diphosphate is noncompetitive. The absence of uncompetitive inhibition patterns supports the notion that the forward reaction is random, while the observation of a noncompetitive pattern when a competitive one is expected is consistent with a steady-state mechanism.

Reverse Reaction. The reverse reaction is expected to be random since product inhibition studies and equilibrium binding studies (Dean *et al.*, 1989) demonstrate that α-ketoglutarate and NADPH each bind to the free enzyme. The random sequential ter mechanism described by eq 5 was fitted

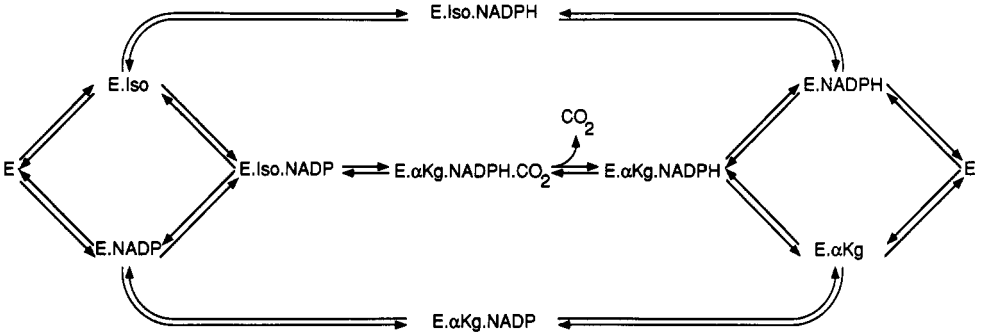

FIGURE 3: Full steady-state random mechanism of wild-type S113 IDH.

to the initial rate data. Ordered ter reactant mechanisms can be diagnosed by the absence of terms in eq 5 (Cleland, 1982). Partial regression analyses, deleting each of the terms constant/V, (coeff P)/V, (coeff Q)/V, (coeff R)/V, K_p/V, K_q/V, K_r/V, and $1/V$ from eq 5 in reciprocal form, show that each coefficient makes a significant contribution to the overall fit. Thus, the reverse reaction has a random mechanism.

Product inhibition studies using (2*R*,3*S*)-isocitrate or NADP yield the two competitive and two noncompetitive inhibition patterns typical of a random mechanism with two abortive complexes (Table III). Dead-end inhibition studies reveal that adenosine 2′,5′-diphosphate is a competitive inhibitor of NADPH and a noncompetitive inhibitor of α-ketoglutarate, whereas tricarballylate yields noncompetitive patterns toward NADPH and α-ketoglutarate (Table III). The absence of uncompetitive inhibition patterns supports the notion that the reverse reaction catalyzed by IDH is random.

However, these results do not distinguish between two kinds of random mechanism—a completely random one and a partially random one in which substrates Q and R add randomly in a steady-state fashion and then P finally binds to form a catalytic complex. The apoenzyme and isocitrate binary complex structures (Hurley *et al.*, 1989, 1990) show no evidence for a specific CO_2 binding pocket, which suggests that a mechanism with CO_2 binding last is the most plausible (Figure 3).

Dissociation Constants. The dissociation constants for NADPH and α-ketoglutarate were calculated from the noncompetitive inhibition patterns of the forward rapid-equilibrium reactions according to the method of Morrison and James (1965). The apparent dissociation constants of NADPH for the wild-type enzyme are 0.007 mM (malate and NADP as substrates) and 0.014 mM (isocitrate and NAD as substrates). These are smaller than the K_{NADPH} = 0.035 mM of the reverse reaction (Table II). The calculated dissociation constant of NADPH from the E·Iso·NADPH complex, K_{Ip} = 0.035, is similar to the dissociation constant of 0.045 mM in the presence of excess isocitrate determined by equilibrium binding experiments (Dean *et al.*, 1989). The estimates of K_{ip} and K_{Ip} for the dissociation of α-ketoglutarate from the E·αKg and E·αKg·NAD complexes are consistent with the values of the $K_{\alpha Kg}$ and Michaelis constants obtained from the reverse reaction (Table II). Although the values are much lower than the E·αKg dissociation constant of 12 mM determined using binding studies (Dean *et al.*, 1989), the direct estimate is suspect because of technical difficulties in estimating an equilibrium dissociation constant in the millimolar range when the enzyme concentration lies in the micromolar range.

Conclusion. Initial rate studies, product inhibition studies, and dead-end inhibition studies of both forward and reverse reactions, together with the use of mutant enzymes, alternative substrates, and equilibrium binding studies, demonstrate unambiguously that the wild-type NADP-dependent IDH of *E. coli* catalyzes a steady-state random mechanism in both directions and that the abortive complexes E·Iso·NADPH and E·αKg·NADP can form (Figure 3).

ACKNOWLEDGMENT

We wish to thank W. W. Cleland, Jack Kirsch, and an anonymous reviewer for their valuable suggestions which so markedly improved the manuscript.

REFERENCES

Apps, D. K. (1973) *Biochim. Biophys. Acta 320*, 379–387.
Burton, K. (1959) *Biochem. J. 71*, 388–395.
Buzdygon, B. E., Braginski, J. E., & Chung, A. E. (1973) *Arch. Biochem. Biophys. 159*, 400–408.
Cleland, W. W. (1963) *Biochim. Biophys. Acta. 67*, 188–196.
Cleland, W. W. (1970) in *Enzymes (3rd Ed.)* (Boyer, P. D., Ed.) Vol. II, pp 1–65, Academic Press, New York.
Cleland, W. W. (1979) *Methods Enzymol. 63*, 500–513.
Cleland, W. W. (1982) *Methods Enzymol. 87*, 353–366.
Dawson, R. M. C., Elliot, D. C., Elliot, W. H., & Jones, K. M. (1969) in *Data for Biochemical Research*, 2nd Ed., Clarendon Press, Oxford, England.
Dean, A. M., & Koshland, D. E., Jr. (1990) *Science 249*, 1044–1046.
Dean, A. M., Lee, M. H. I., & Koshland, D. E., Jr. (1989) *J. Biol. Chem. 264*, 20482–20486.
Duggleby, R. G., & Dennis, D. T. (1970) *J. Biol. Chem. 245*, 3745–3754.
Erhlich, R. S., & Colman, R. F. (1987) *Biochemistry 26*, 2461–2471.
Grissom, C. B., & Cleland, W. W. (1988) *Biochemistry 27*, 2934–2943.
Haselbeck, R. J., & McAlister-Henn, L. (1991) *J. Biol. Chem. 266*, 2339–2345.
Head, E. J. H. (1980) *Eur. J. Biochem. 111*, 581–586.
Huang, C. Y. (1979) *Methods Enzymol. 63*, 486–500.
Hurley, J. H., Thorsness, P., Ramalingham, V., Helmers, N., Koshland, D. E., Jr., & Stroud, R. M. (1989) *Proc. Natl. Acad. Sci. U.S.A. 86*, 8635–8639.
Hurley, J. H., Dean, A. M., Stohl, J. L., Koshland, D. E., Jr., & Stroud, R. M. (1990) *Science 249*, 1012–1016.
Hurley, J. H., Dean, A. M., Koshland, D. E., Jr., & Stroud, R. M. (1991) *Biochemistry 30*, 8671–8678.
Lienhard, G. E., & Rose, I. A. (1964) *Biochemistry 3*, 185–190.
Londesborough, J. C., & Dalziel, K. (1968) *Biochem. J. 110*, 217–222.
Londesborough, J. C., & Dalziel, K. (1970) in *Pyridine Nucleotide Dependent Dehydrogenases, Proceedings of the Advanced Study Institute* (Sund, H., Ed.) pp 315–323, Springer-Verlag, Berlin.

Marr, J. J., & Weber, M. M. (1973) *Arch. Biochem. Biophys. 158*, 782–791.
Morrison, J. F., & James, E. (1965) *Biochem. J. 97*, 37–52.
Nimmo, H. G. (1986) *Biochem. J. 234*, 317–323.
Northrop, D. B., & Cleland, W. W. (1974) *J. Biol. Chem. 249*, 2928–2931.
Reeves, H. C., Daumy, G. O., Lin, C. C., & Houston, M. (1972) *Biochim. Biophys. Acta 258*, 27–39.
Rossmann, M. G., Moras, D., & Olsen, K. W. (1974) *Nature 250*, 194–199.
Rudolph, F. B., and Fromm, H. J. (1971) *J. Biol. Chem. 246*, 6611–6617.
Siebert, G., Carsiotis, M., & Plaut, G. W. E. (1957) *J. Biol. Chem. 226*, 977–991.
Steinberger, R., & Westheimer, F. H. (1951) *J. Am. Chem. Soc. 73*, 429–435.
Thompson, L. M., Sutherland, P. A., Steffan, J. S., & McAlister-Henn, L. (1988) *Biochemistry 27*, 8393–8400.
Uhr, M. L., Thompson, V. W., & Cleland, W. W. (1974) *J. Biol. Chem. 249*, 2920–2927.
Wicken, J. S., Chung, A. E., & Franzen, J. S. (1972) *Biochemistry 11*, 4766–4788.
Willson, V. J. C., & Tipton, K. F. (1981) *Eur. J. Biochem. 113*, 477–483.